Nanoscale

Accepted Manuscript

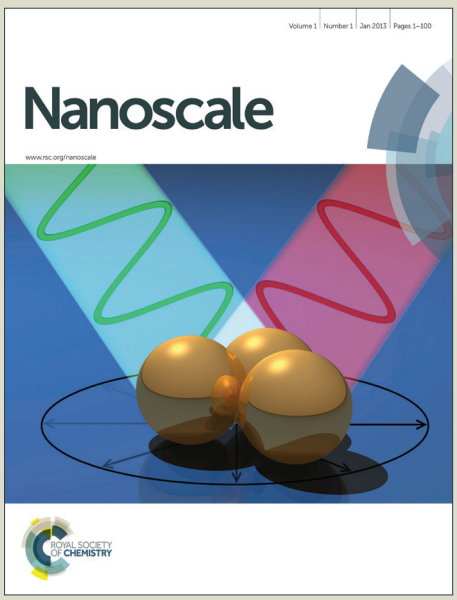

ROYAL SOCIETY OF CHEMISTRY

www.rsc.org/nanoscale

Journal Name

RSCPublishing

COMMUNICATION

Criticality of Surface Topology for Charge-carrier Transport Characteristics in Two-Dimensional Borocarbonitrides: Design Principle of an Efficient Electronic Material

Swastika Banerjee,[a,b] *and Swapan K. Pati**[a,b,c]

[a]New Chemistry Unit,

[b]Jawaharlal Nehru Center for Advanced Scientific Research, Bangalore 560064, India

[c]Theoretical Sciences Unit

E-mail: swapan.jnc@gmail.com

KEYWORDS: Electronic transport, Mobility, Borocarbonitride sheet, Density functional theory, Boltzmann transport,

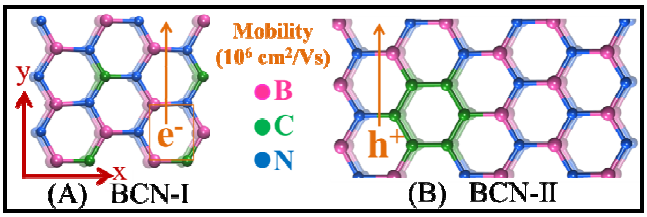

We have studied the effect of spatial distribution of BN and C domains in 2-dimensional borocarbonitrides and its influence on the carrier mobility, based on density functional theory coupled with Boltzmann transport equation. Two extreme features of C-domains in BN-rich $B_{2.5}CN_{2.5}$, namely BCN-I (random) and BCN-II (localized) have been found to exhibit the electron (hole) mobility as ~10^6 cm^2/Vs (~10^4 cm^2/Vs) and ~10^3 cm^2/Vs (~10^6 cm^2/Vs) respectively. We ascertain the underlying microscopic mechanisms behind such extraordinarily large carrier mobility and the reversal of conduction polarity. Finally, we derive the principle for maximizing mobility and obtaining particular (electron/hole) conduction polarity of this nano-hybrid at any stoichiometric proportion.

Semiconducting electronic material shoulders both the functions (i) the task of light absorption and (ii) charge carrier transport. Sensing light and electron field emissions are the properties attributed to the optical and electronic band gap in semiconductors. On the other hand, the power factor of electronic devices depends on the carrier transport property and current conversion efficiency. Popular electronic material graphene (single layer), shows very high carrier mobility (~1.5×10^4 cm^2/Vs at room temperature) [1] due to the presence of massless Dirac Fermions. However, in spite of this large carrier mobility, gapless semi-metallic nature limits its performance as a versatile electronic material. This has driven the search for graphene analogues wherein certain shortcomings of graphene could be compensated.[2-5] Fascinatingly, hexagonal-BN sheet (h-BN) exhibits large optical phonon modes, large electronic band gap (~5.97 eV) but poor intrinsic carrier mobility due to the charge traps on B and N atoms.[6, 7] Now-a-days, moderate carrier mobility coupled with suitable electronic band gap has been tried through the optimization between carbon (responsible for good electrical conductivity) and B, N (acting as redox centers) concentration.[8-10] In fact, borocarbonitrides with combination of sensible carrier mobility (10^2-10^3 cm^2/Vs) and finite band gap find application in electron field-emission, electrocatalysis, [11] supercapacitor.[12, 13] and modern day electronic devices.[14, 15] On the other hand, p or n-type conduction polarity have been controlled through electrochemical doping, surface adsorption, chemical functionalization and lattice symmetry breaking. For the back-gate field-effect transistors, B doping in graphene have been found to exhibit p-type behaviour and lower electron mobility (350–550 cm^2/Vs) than its N-doped analogue (450–650 cm^2/Vs).[16, 17] But, there are also practical difficulties associated with poor mobility and in preserving the doping state in ambient environment.[18] This push us toward fundamental limits, demands in-depth understanding of how surface structure and the interface affect the carrier mobility in borocarbonitride nano-hybrids.

In this communication, we notify whether the topological modification in borocarbonitrides can be a promising approach to address these issues, as the properties controlled by surface topology are arguably more robust against an external

polarization and electrochemical oxidation/reduction with respect to the doping and other tactics. In fact, sustainable electrochemical performance (100 mA h g^{-1} at 2 A g^{-1} for 5000 cycles with capacity retention of 93 %) of $B_{2.5}CN_{2.5}$ have been found by W. Lei *et al.* [14] This reflects the stability of the material even at high current rate, speaks of its high intrinsic carrier mobility. We discuss the carrier transport characteristics and the topological criticality in monolayer and bilayer $B_{2.5}CN_{2.5}$ (see abs fig and Fig. 1). Understanding on the surface electronic structure and basic transport mechanism has been applied to determine an efficient material-design for electronic devices and electrochemical applications. Apart from this particular composition we have also considered two recently highlighted[19, 20] carbon-rich compositions (see Fig. 2; BCN and BC_4N and applied the principle discussed in this manuscript. This investigation would not only of fundamental academic interest; it would also be of great technical relevance in modern electronic devices and energy storage.

$B_{2.5}CN_{2.5}$ composition results in various possible surface structures as shown in abstract figure and Fig. S1 in supporting information (S.I.). Moreover, the re-stacking of layered material is one of our concerns for device applications. Hence, structural analysis becomes relevant to address the importance of various stacking patterns and to have the preliminary information aimed at our further

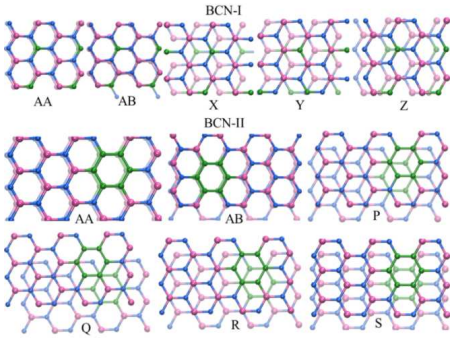

Fig. 1. Top view of the various stacking patterns including bilayer $B_{2.5}CN_{2.5}$; namely BCN-I: AA,AB,X,Y,Z; BCN-II: AA,AB,P,Q,R,S. The pink spheres represent B atoms, and the green and blue spheres represent C and N atoms respectively.

investigation on carrier transport characteristics. From outcomes of the Density functional theory (DFT) [21-24] and *Ab* initio molecular dynamic (AIMD)[25, 26] simulations (NVT; 300 K,) (see S.I. for computational details), it is revealed that, the surface topology viable to model BCN-I (ID = 0.33nm) is in good qualitative and quantitative agreement with the experimental x-ray measurements [5]. The B, C and N atoms are positioned so that each and every hexagonal ring contains one C atom only so that it is truly mixed or random (see BCN-I). In contrast, we also account for (see BCN-II and Fig. S1.C, D) another model surface structures with localized C-domain, showing well agreement with previous theoretical studies and experimental evidences[12, 15] (ID ~ 0.40nm). Based on the relative energy (RE; energy of any stacking pattern with respect to the most stable

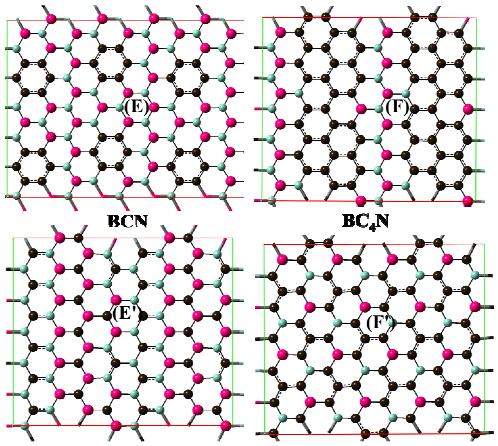

stacking arrangement) and cohesive energy (CE; the estimate of the stability gained due to the bilayer formation) we determine the most stable stacking pattern for BCN-I and II (see Table 1).

Fig. 2. (E) Equi-separated localized C-domains in BCN and (F) is the same for BC_4N. E' and F' are corresponding random B,C and N distributions for BCN and BC_4N respectively.

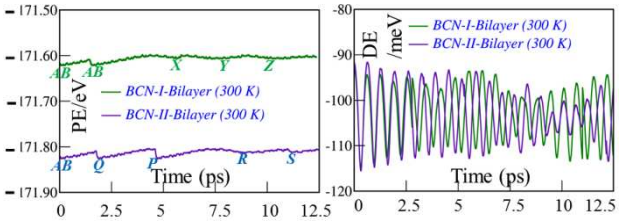

Fig. 3. Potential Energy (PE) vs Time (left) and Dispersion Energy (DE) vs Time (right) plots for bilayer BCN-I and BCN-II with PBE-D2 approaches[27]

Table 1. Relative energy (RE), interlayer distance (ID) and cohesive energy (CE) of various stacking pattern of bilayer BCN-I and BCN-I have been shown.

Sheet	RE	ID	CE
BCN-I-AA	19.385	3.66	-17.264
BCN-I-AB	0.000	3.46	-36.649
BCN-I-X	5.107	3.63	-31.542
BCN-I-Y	6.777	3.50	-29.871
BCN-I-Z	8.842	3.63	-27.807
BCN-II-AA	14.290	3.70	-19.194
BCN-II-AB	3.070	3.55	-30.414
BCN-II-P	0.000	3.62	-33.484
BCN-II-Q	1.855	3.43	-31.629
BCN-II-R	2.095	3.45	-31.390
BCN-II-S	4.988	3.42	-28.496

The difference in stability is quite less for different stacking patterns in either of the surface topology (see Table 1 and Fig. 3) at both low (0K) and room temperature (300K) and the stability remains for a long time window. This reveals that, these stacking arrangements are highly feasible at ambient conditions. Moreover, DE vs Time plot helps to figure out the role of dispersion force on the structural integrity, favorable stacking pattern and equilibrium separation distances between two layers in various stacking arrangements. From comparative analysis of two different sheets, BCN-II-AB have

been found to be energetically more stable (diff: ~0.207 eV/atom) than BCN-I-AB.

Next, we use this structural analysis and sample the energetically stable bilayer stacking patterns (BCN-I-AB and BCN-II-AB) to study the transport characteristics. In this work, charge-carrier mobility (μ) is evaluated based on the Boltzmann transport formalism within the Deformation Potential (DP) theory. [28, 29]

$$\mu_{\alpha}^{e(h)} = \frac{e}{k_B T} \frac{\sum_{i\in CB(VB)} \int \tau_{\alpha}(i,\vec{k}) v^2{}_{\alpha}(i,\vec{k}) \exp\left[\mp \frac{\varepsilon_i(\vec{k})}{k_B T}\right] d\vec{k}}{\sum_{i\in CB(VB)} \int \exp\left[\mp \frac{\varepsilon_i(\vec{k})}{k_B T}\right] d\vec{k}} \quad Equation(1)$$

		Monolayer				Bilayer			
Sheet	Carrier type	E_1 (eV)	C^{β} (J/m^2)	μ (10^4 cm^2/V s)	τ(ps)	E_1 (eV)	C^{β} (J/m^2)	μ (10^4 cm^2/V s)	τ(ps)
A	e^x	3.74	297.88	0.82	1.16	2.42	598.28	7.28	10.62
	h^x	1.76	297.88	3.27	5.34	1.76	598.28	11.8	19.15
	e^y	0.44	285.57	56.75	80.40	0.44	575.69	212.04	309.12
	h^y	2.86	285.57	1.39	2.78	1.32	575.69	20.22	32.76
B	e^x	3.96	302.14	0.13	0.79	3.30	618.98	0.33	1.81
	h^x	0.66	302.14	8.65	49.29	1.76	618.98	1.59	6.86
	e^y	3.74	302.39	0.15	0.89	3.30	616.23	0.32	1.80
	h^y	1.54	302.39	1.59	9.06	0.22	616.23	101.08	436.91

Where, α denotes the direction of external field and the minus (plus) sign is for electron (hole). $\varepsilon_i(\vec{k})$ and $v_{\alpha}(i,\vec{k})$ are band energy and the α component of group velocity at $\vec{k}$ state of the *i*th band, respectively. The summation of band was carried out over valence band (VB) for hole and conduction band (CB) for electron. Furthermore, the integral of $\vec{k}$ states is over the first Brillouin Zone (BZ), where the band energy $\varepsilon_i(\vec{k})$ was obtained from density functional theory. We note that, acoustic phonon mechanism and deformation potential theory can well explain the charge transport behavior in graphene nanoribbons too.[30] The relaxation time $\tau_{\alpha}(i,\vec{k})$ is calculated by the collision term in the Boltzmann method.[31] Using deformation potential formalism, $\tau_{\alpha}(i,\vec{k})$ is expressed as

$$\frac{1}{\tau_{\alpha}(i,\vec{k})} = k_B T \frac{4\pi^2 E_1^{\,2}}{hC^{\beta}} \sum_{K'\in BZ} \left\{ \left(1 - \frac{v_{\alpha}(\vec{k}')}{v_{\alpha}(\vec{k})}\right) \delta[\varepsilon_i(\vec{k}') - \varepsilon_i(\vec{k})] \right\} Equation(2)$$

E_1 is the deformation potential constant of the *i*-th band, and C^{β} is the elastic constant along the direction β.

Inputs to this analysis have been derived from first principles calculations based on density functional theory as implemented in Vienna ab initio simulation package (VASP). [21-24] Further details on computational method have been provided in the supporting information. Band structure calculation relates BCN-I as narrow band gap (~0.45 eV at the Γ-point) while, BCN-II as wide band gap (~2.80 eV at the Γ-point) semiconductor (see Fig S2 in S.I.).

Table 2. Deformation Potential E1, Elastic Constant Cβ, Carrier Mobility μ, and the Averaged Value of Scattering Relaxation Time τ at 300 K for electrons and holes in monolayer and bilayer borocarbonitrides (B2.5CN2.5)

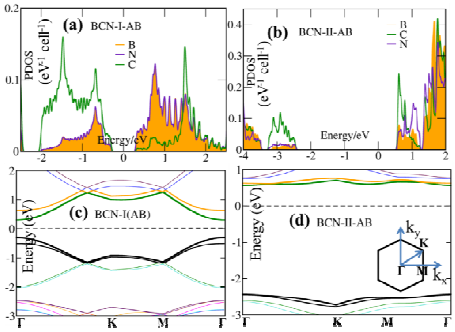

with different surface topologies (A:BCN-I and B:BCN-II).

We find that, for bilayer BCN-I, the intrinsic electron mobility (see Table 2) reaches up to the order of 10^6 cm^2/Vs along y-direction (y: two consecutive C atoms are non-collinear; separated by one BN bond). On the other hand, bilayer BCN-II exhibits reversal of conduction polarity showing high hole-mobility (~ 10^6 cm^2/Vs) along y-direction (y: two hexagonal C-domains are periodically separated by 3 B/N atoms (odd number; either an extra electron or an extra hole)). Electronic structural calculation reveals that, for BCN-I, the CBM is delocalized due to the diffused nature of N 2pz orbitals (see Fig. 4) and shows lesser number of nodes along y-direction. This leads to weak coupling between the electron and the acoustic phonons, reducing the effective scattering and enhances the electron mobility of BCN-I. On the other hand, in CBM of BCN-II, carbon hexagons and BN-domains combine anti-symmetrically (anti-bonding feature), while the VBM consists of bonding (symmetric) features with the appearance of kink states at N sites, acting as a connector between two diffused electronic islands. It is noteworthy; the kink states appear on N site in VBM always when localized C-domains form ((see Fig. 5. I. (B,C ans D) and II.B). These topologically protected kink states are, in fact, needed to maintain the connectivity between two C-domains, so that, the number of nodes in VBM decreases and the position-dependent masses get modulated. This results in enormous hole-mobility. Apart from BCN-II, we have considered two other topological effects; unequal separations (see Fig S1.C) and long bridging B-N chain (seven atoms) (see Fig S1.D) between localized C-domains. Either of these ways lowers the hole conductivity (see Table T1 in S.I.) revealing the fact that not only localization of C-domains but also the relative separation among them plays an important role in hole transport efficiency. Thus, with extensive calculations on a number of these systems, we find two critical conditions for achieving highest electron and hole mobility, the requirements are: (i) topological features like BCN-I type (C atoms to be perfectly randomized) and BCN-II type (equidistant localized C-domains with the least possible separation) respectively.

Fig. 4. Band structure and projected density-of-states of states for bilayer borocarbonitride ($B_{2.5}CN_{2.5}$) sheet in their stable stacking pattern are obtained from DFT calculations. Both of them exhibit direct band gap. The inset displays the first Brillouin zone of the primitive cell with three high symmetry points Γ, K, and M.

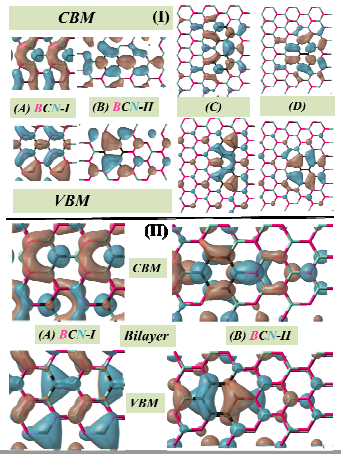

Fig. 5. Γ-point VBM and CBM for model surface topologies; (I) monolayer (II) bilayer have been shown. I. (A) CBM consists of more extended islands than the VBM. The number of nodes in VBM is equal in either direction. I. (B), (C) and (D); VBM exhibits more delocalized character than CBM along y-direction and kink states appears on N atom. I. (C) and (D) plots are for the surface structures described in Fig S1.C and D respectively.

Another aspect is, irrespective of the surface topology, the carrier mobility gets enhanced in bilayer structure (compared to monolayer, see Table 2) for either of the charges. To understand the effect of layers, we analyze each of the terms in eq. 1, contributing to mobility. We find that, relaxation time (τ) value changes significantly from monolayer to bilayer. This echoes the importance of subsurface scattering (see eq. 2). Significant contribution of 2pz orbitals of C, B and N (perpendicular to the transport plane) to both the CBM and VBM (see Fig S3 in S.I.) gives rise to alteration in the E_1 (eV) values in layered structure. Hence, the modulation in carrier transport property in layered structure is due to electronic structural changes leading to phonon softening. This corroborates with previous observation on anomalous phonon softening in case of bilayer graphene.[32]

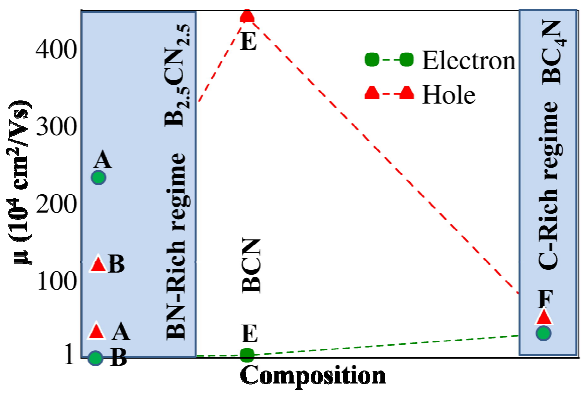

Fig. 6. Carrier Mobility μ, for electrons and holes in borocarbonitrides ($B_xC_yN_z$) with different stoichiometric proportion of B,C and N (different surface topologies are A:BCN-I, B:BCN-II, E:BCN, F:BC_4N).

We also have studied the composition dependence of the intrinsic carrier mobilities. Unlike BN predominant composition ($B_{2.5}CN_{2.5}$), C-rich compositions (BCN and BC_4N) with truly random surface structure (see Fig. 2 E',F') drives the material to be metallic that well corroborates with previous studies[19, 20]. On the other hand, the stable surface with localised C-domains are semiconducting in nature (see Fig. 2 E, F). Extremely high hole mobility (~10^6 cm^2/Vs) but comparatively poor e-mobility in BCN (~10^4 cm^2/Vs) is found (see Fig. 6 and Table T1 in S.I.), using the the same formalism discussed earlier. BC_4N exhibits both the electron and hole mobility in the order of ~10^5 cm^2/Vs which is attributed to the equalization of both hole and electronic relaxation time (see Fig. 6 and Table T1 in SI). Hence, extended C-domains lead to equalization of intrinsic hole and electron mobility. This is because in this case compensation of the electron mobility occurs at the cost of hole mobility.

In conclusion, we would like to stress that BN-rich borocarbonitrides ($B_{2.5}CN_{2.5}$) are semiconducting in nature irrespective of surface topology and (i) the random mixing of BN and C (BCN-I) is energetically less stable than localized domains (BCN-II). Thus, the topological feature of BCN-I can be defined as topological defect in stable surface of type BCN-II. These topological defects give rise to extremely high electronic mobility, thereby higher rate performance by a factor of 10^3 in comparison with most stable topological feature. (ii) Electronic confinement becomes dominant and transport channels have directional behaviour. Moreover, for a particular composition, electronic bandgap can be varied within a wide range (0.45 to 2.8 eV) of energy spectrum depending on the surface topology. (iii) Reversal of the conduction polarity[28] has also been found with the change in surface topology. The leading carrier transport in transistors can be changed from electrons (for BCN-I) to holes (for BCN-II) with high mobility value (μ = 10^6 cm^2/Vs). Extreme electron mobility can be reached for surface structure with random (truly mixed) C atoms in BN matrix (model BCN-I). In contrary, hole mobility becomes extremely high and more robust when localized C-domains (see BCN-II model structure) are at closest as well as equidistant (periodically situated). The principles analyzed turn out not to be specific to $B_{2.5}CN_{2.5}$, but can be extended to borocarbonitrides with different stoichiometric proportions too. This understanding can lead to the optimization of the atomically engineered surface topology to tailor low-dimensional carrier transport mobility and develops fundamental in designing a smart material for modern day electronic (transport) and energy storage devices.

Supporting Information Available: Additional Figures and Tables, as referred in main-text.

S.B. would like to acknowledge CSIR, Govt. of India for a senior research fellowship and S.K.P. acknowledges DST (Government of India) for a research grant.

1. K. S. A. Novoselov, A. K. Geim, S. Morozov, D. Jiang, M. I. K. I. V. Grigorieva, S. V. Dubonos and A. A. Firsov, *nature*, 2005, **438**, 197-200.
2. M. Y. Han, B. Ã¯zyilmaz, Y. Zhang and P. Kim, *Physical review letters*, 2007, **98**, 206805.
3. H. S. S. Ramakrishna Matte, A. Gomathi, A. K. Manna, D. J. Late, R. Datta, S. K. Pati and C. N. R. Rao, *Angewandte Chemie*, 2010, **122**, 4153-4156.
4. G. Giovannetti, P. A. Khomyakov, G. Brocks, V. M. Karpan, J. Van den Brink and P. J. Kelly, *Physical review letters*, 2008, **101**, 026803.
5. S. Banerjee, G. Periyasamy and S. K. Pati, *Journal of Materials Chemistry A*, 2014, **2**, 3856-3864.
6. K. Watanabe, T. Taniguchi and H. Kanda, *Nature materials*, 2004, **3**, 404-409.
7. G. Giovannetti, P. A. Khomyakov, G. Brocks, P. J. Kelly and J. van den Brink, *Physical Review B*, 2007, **76**, 073103.
8. S. Dutta, A. K. Manna and S. K. Pati, *Physical review letters*, 2009, **102**, 096601.
9. D. Wei, Y. Liu, Y. Wang, H. Zhang, L. Huang and G. Yu, *Nano letters*, 2009, **9**, 1752-1758.
10. C. R. Dean, A. F. Young, I. Meric, C. Lee, L. Wang, S. Sorgenfrei, K. Watanabe, T. Taniguchi, P. Kim and K. L. Shepard, *Nature nanotechnology*, 2010, **5**, 722-726.
11. L. Qu, Y. Liu, J.-B. Baek and L. Dai, *ACS nano*, 2010, **4**, 1321-1326.
12. N. Kumar, K. Moses, K. Pramoda, S. N. Shirodkar, A. K. Mishra, U. V. Waghmare, A. Sundaresan and C. N. R. Rao, *Journal of Materials Chemistry A*, 2013, **1**, 5806-5821.
13. K. Gopalakrishnan, K. Moses, A. Govindaraj and C. N. R. Rao, *Solid State Communications*, 2013, **175**, 43-50.
14. W. Lei, S. Qin, D. Liu, D. Portehault, Z. Liu and Y. Chen, *Chemical Communications*, 2013, **49**, 352-354.
15. S. Sen, K. Moses, A. J. Bhattacharyya and C. N. R. Rao, *Chemistryâ€ "An Asian Journal*, 2014, **9**, 100-103.
16. H. Wang, Y. Zhou, D. Wu, L. Liao, S. Zhao, H. Peng and Z. Liu, *small*, 2013, **9**, 1316-1320.
17. T. Wu, H. Shen, L. Sun, B. Cheng, B. Liu and J. Shen, *New Journal of Chemistry*, 2012, **36**, 1385-1391.
18. B. J. Cho, J. H. Bong, O. Sul, A. Yoon and S. Y. Choi, *Nanoscale*, 2014.
19. K. Raidongia, D. Jagadeesan, M. Upadhyay-Kahaly, U. V. Waghmare, S. K. Pati, M. Eswaramoorthy and C. N. R. Rao, *J. Mater. Chem.*, 2008, **18**, 83-90.
20. K. Moses, S. N. Shirodkar, U. V. Waghmare and C. N. R. Rao, *Materials Research Express*, 2014, **1**, 025603.
21. G. Kresse and J. r. Hafner, *Physical Review B*, 1993, **47**, 558.
22. G. Kresse and J. Hafner, *Physical Review B*, 1994, **49**, 14251.
23. G. Kresse and J. r. FurthmÃ¼ller, *Computational Materials Science*, 1996, **6**, 15-50.
24. G. Kresse and J. r. FurthmÃ¼ller, *Physical Review B*, 1996, **54**, 11169.
25. J. VandeVondele, M. Krack, F. Mohamed, M. Parrinello, T. Chassaing and J. r. Hutter, *Computer Physics Communications*, 2005, **167**, 103-128.
26. J. r. Hutter, M. Iannuzzi, F. Schiffmann and J. VandeVondele, *Wiley Interdisciplinary Reviews: Computational Molecular Science*, 2013, **4**, 15-25.
27. S. Grimme, *Journal of computational chemistry*, 2006, **27**, 1787-1799.
28. J. Bardeen and W. Shockley, *Physical Review*, 1950, **80**, 72.
29. Y. C. Cheng, R. J. Silbey, D. A. da Silva Filho, J. P. Calbert, J. Cornil and J.-L. BrÃ©das, *The Journal of chemical physics*, 2003, **118**, 3764-3774.
30. M.-Q. Long, L. Tang, D. Wang, L. Wang and Z. Shuai, *Journal of the American Chemical Society*, 2009, **131**, 17728-17729.
31. J. M. Ziman, *Principles of the Theory of Solids*, Cambridge university press, 1972.
32. J. Yan, E. A. Henriksen, P. Kim and A. Pinczuk, *Physical review letters*, 2008, **101**, 136804.

TOC GRAPHICS: Computational investigation based on *ab*-initio density functional theory combined with Boltzmann transport enlightens the principles for maximizing mobility and possibility for obtaining particular (electron/hole) conduction polarity of borocarbonitrides. This understanding develops fundamental in designing a smart material for modern day electronic (transport) and energy storage devices.